MICROOPTICS DESIGN TECHNIQUE AND ITS APPLICATION TO OPTICAL DEVICES FOR DWDM

SANPEI Yoshihiro [*1] ***SUZUKI Yasuyuki*** [*2] ***IEMURA Kouki*** [*3] ***ASANO Junichirou*** [*3]

This paper describes a compact optical channel monitor and a delayed interferometer having free-space optical elements such as lenses or mirrors, as an application of microoptics. These devices have been developed to be built into dense wavelength division multiplexing (DWDM) transmission systems. These optics use a Gaussian beam which is emitted through single-mode optical fibers and located near the optical axis. This paper explains the optical designs of these devices based on the Gaussian beam's behavior.

INTRODUCTION

Microoptics covers a wide range of fields including optical generation, amplification, transmission, concentration, imaging, branching and so on. It involves units or optical devices which are integrated with or assembled microoptic elements, and also refers as general technologies based on such units or devices. The applications of microoptics encompass optical fiber communication, optical disk memory, and optical measurement[(1)(2)(3)].

There are two approaches for making the elements much smaller: one is using waveguide devices, and the other is using free-space optical devices such as a lens and mirror. The former devices have a constraint of design flexibility and materials, however, some elements such as highspeed modulators can take full advantage of thier optical charactoristics. The latter aims to make the optics smaller, simpler, and more integrated by taking advantage of coherent light that is emitted from an optical fiber or semiconductor laser, and that is highly coherent in time and space and localized around the optical axis.

This paper describes a compact optical channel monitor and a delay interferometer using the latter approach. Both instruments have been developed and commercialized as optical communication devices. The light beam is a Gaussian beam whose amplitude distributions in the electric field from a single-mode optical fiber are categorized as Gaussian distribution and localized around the optical axis. Its features and impact on the performance of optical systems are also described.

*1 Communication and Measurement Business Headquarters, Optical Communication Measurement Development Department
*2 Communication and Measurement Business Headquarters, Core Technology Development Department
*3 Photonics Business Headquarters, Engineering Department IV

GAUSSIAN BEAM PROPAGATION

First, we briefly explain about Gaussian beam. Optical field distributions at the end of optical fibers are described by two functions: Bessel function J_0 in the fiber core, and modified Bessel functions of the second kind K_0 in the cladding. An output beam of light is approximated by a Gaussian beam having the beam waist, which is the beam's narrowest point, at the end of the optical fiber. The field distribution at the end of an optical fiber is given by: (the following formulas (1) to (6) are from reference No.(4) and (5))

$$u = \frac{\omega_0}{\omega(z)} \exp\left[-\frac{r^2}{\omega(z)^2}\right] \exp\left[-j\frac{kr^2}{2R(z)}\right] \times \exp\left[-jkz + j\tan^{-1}\left[\frac{z}{z_0}\right]\right] \quad \cdots (1)$$

where z is the vertical direction, r is the radial distance from the center axis of the beam, λ is the wavelength at the point r, $\omega(z)$ is the radius of the beam, $R(z)$ is the radius of curvature of the wavefront, and z_0 is the Rayleigh length.

$\omega(z)$, $R(z)$, and z_0 are given by:

$$\omega(z) = \omega_0\sqrt{1+(z/z_0)^2}$$

$$R(z) = z\,(1+(z_0/z)^2) \quad \cdots(2)$$

$$z_0 = \pi\omega_0{}^2/\lambda$$

where $\omega(z)$ is the distance from the center axis to the point at which the intensity falls to $1/e^2$ of its axial value (the peak value), and ω_0 is the spot size (the radius at the beam waist).

The radius of the beam increases gradually at first with increase in the value of z, then eventually increases in proportion to z. The radius of curvature of the wavefront, which is an infinite value at the first point where $z = 0$, decreases gradually into an finite value with increase in the value of z, then eventually increases in direct proportion to z again.

The outgoing beams are explained in the above paragraphs. This theory, however, can apply to the case where the direction of a Gaussian beam is reversed. This means that using a lens, it is possible to narrow down a Gaussian beam whose beam radius is large. With the lens features, a Gaussian beam is converted to the following easy input/output relations by the optical system which can be described by the ray transfer matrix (the ABCD matrix).

$$q_2 = \frac{Aq_1 + B}{Cq_1 + D} \quad \cdots(3)$$

where q_1 and q_2 are respectively an input and output complex beam parameter, given by:

$$\frac{1}{q} = \frac{1}{R(z)} - j\frac{\lambda}{\pi\omega(z)^2} \quad \cdots(4)$$

If q_1 and ω_1 are respectively an input complex beam parameter and spot size at the beam waist (the radius of wavefront curvature is infinite), and q_2 and ω_2 are respectively an output complex beam parameter and spot size at the beam waist, then the following formulas are obtained:

$$q_1 = j\frac{\pi\omega_1{}^2}{\lambda},\ q_2 = j\frac{\pi\omega_2{}^2}{\lambda} \quad \cdots(5)$$

$$AC + BD\left[\frac{\lambda}{\pi\omega_1{}^2}\right]^2 = 0$$

$$\omega_2{}^2 = \omega_1{}^2\left\{A^2 + B^2\left[\frac{\lambda}{\pi\omega_1{}^2}\right]^2\right\} \quad \cdots(6)$$

When these formulas are applied to the lens system illustrated in Figure 1, for example, the size of the spot ω_1 on the object side at distance d_1 from the lens and its image spot size ω_2 and distance d_2 can be easily calculated.

Next, to explain the behavior of beam west directly, we introduce variable α, which is the distance from the position to the focal plane normalized by the Rayleigh length. Let α be written as:

$$d_1 - f = \alpha\frac{\pi\omega_1{}^2}{\lambda} \quad \cdots(7)$$

then ω_2 and d_2 are calculated as,

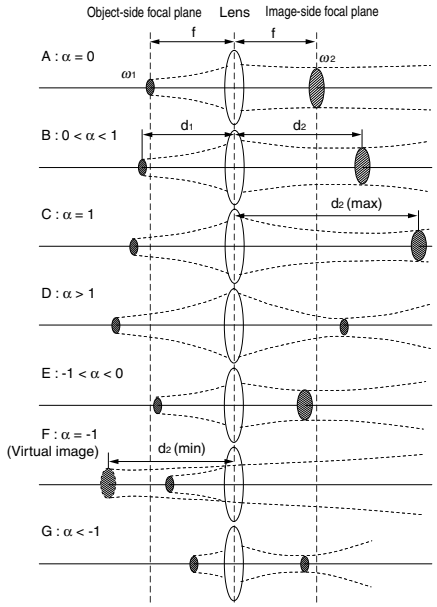

Figure 1 Change of the Beam Waist in the Lens System

$$d_2 - f = \frac{\alpha}{1+\alpha^2}\cdot\frac{\lambda}{\pi\omega_1{}^2}f^2$$

$$\omega_2 = \frac{1}{\sqrt{1+\alpha^2}}\cdot\frac{\lambda}{\pi\omega_1}f \quad \cdots(8)$$

This relation of variables looks simple. Figure 1 shows the relation of $d_2 - f$ and ω_2 to α, and Figure 2 plots the relation as a graph. In general, the formula in which $d_2 - f$ is normalized by f is used[5].

OPTICAL CHANNEL MONITOR

An optical channel monitor (OCM), which is incorporated in a wavelength division multiplexing (WDM) transmission unit, measures the wavelengths of WDM signals, optical power, optical signal-to-noise ratio (OSNR), and so forth. In response to the strong demand for compact, thin and flat optical channel monitors, various optical channel monitors based on different principles are required for practical use.

Yokogawa has released the WD30, the latest model of optical

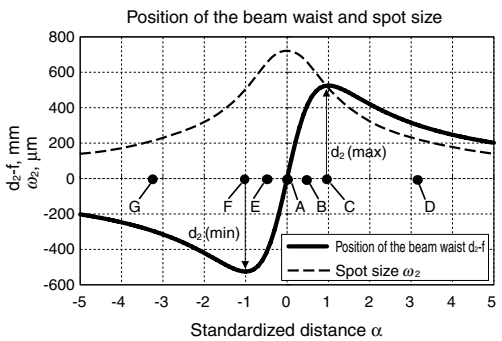

Figure 2 Behavior of the Beam Waist: the Size and Position of ω_2
(f=7 mm, ω_1=4.5 μm, λ=1.55 μm)

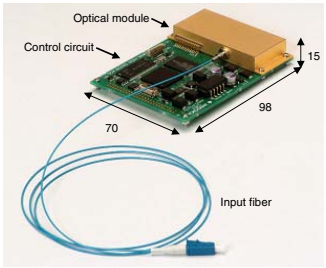

Figure 3 External View of the WD30 Optical Channel Monitor

Table 1 Specifications of the WD30 Optical Channel Monitor

Item	Specification
Measurement Wavelength Range	C or L-band (1528.77-1608.33 nm)
Channel Count	41 (max46)
Channel Spacing	100 GHz (≒0.8 nm)
Measurement Power Range	-10 to -40 dBm
Power Accuracy	+/- 0.5 dB
Wavelength Accuracy	+/- 60 pm
Response Time	< 20 ms
Electronics I/F	DPRAM/RS232C
Dimensions	70 × 98 × 15 mm
Operating Temperature Range	-5 to 65°C

channel monitor, which is a polychromator-based (receiving diffracted light with no moving parts) spectrometer using photodiode array elements and a fixed diffraction grating, resulting in a highly reliable optical channel monitor. The unit is compact and the entire optical system including photodiode element is sealed, thus further boosting reliability. Figure 3 shows an external view of the WD30, and Table 1 lists the main specifications.

Figure 4 shows the optical system of the WD30. To keep sufficient resolution with a compact, thin and flat body, the optical system uses an additive-dispersion configuration in which the light diffracts two times by return.

To obtain ideal diffraction, the wavefront of a light beam incident on a diffraction grating should be a planar wave; that is the beam waist, whose wavefront is planar, must be formed near the diffraction grating. The lens system of the WD30 uses the pseudo-confocal system, which means that the distance from the lens to the diffraction grating is not equal to the focal length, and the case is $\alpha \neq 0$ in Figure 1 and formulas (7) and (8). It is possible to form the beam waist near a diffraction grating, so the WD30 uses this mechanism.

The amplitude of an electrical field has a Gaussian distribution, so the diffraction pattern (spectrum) of a diffraction grating is given

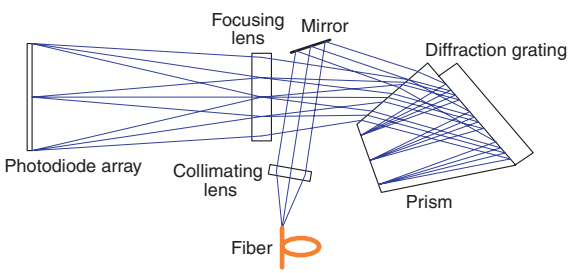

Figure 4 Optical System of the WD30

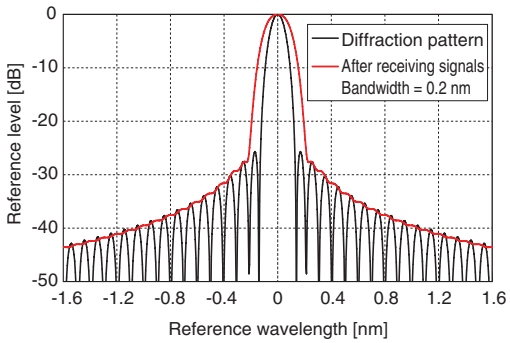

Figure 5 Diffraction Pattern
(Number of grooves of diffraction grating: 6,500 for effective aperture 1.2ω)

by the following formula as the superposition of diffracted beams of light from each groove:

$$P(\lambda) = \left| \sum_{n=-1.2\omega}^{+1.2\omega} \exp\left[-\frac{n^2}{\omega^2}\right] \exp\left[-j2\pi \frac{\lambda}{\lambda_0} n\right] \right|^2 \cdots (9)$$

The diffraction pattern is summed up within $\pm 1.2\omega$ because the effective size of the diffraction grating is 1.2 times the beam diameter 2ω. Figure 5 shows the results of the diffraction pattern and the spectrum received by a detector with a bandwidth of 0.2 nm. The full width at half maximum (FWHM) of the main lobe, which is an index of resolution, matches the actual result. In the Gaussian distribution, the side lobe is suppressed by the result of apodization, so that the optical dynamic range can meet the performance required by an OCM.

The resolution $\Delta\lambda$, which is one of the indexes of the performance of a spectrometer, is expressed by $\Delta\lambda = \lambda/N$ (N: number of effective grooves). Thus, to improve the resolution, the number of grooves of the diffraction grating must be increased by using a large-aperture lens with a long focal length. To maintain a dynamic range, which is another index of the performance of a spectrometer, a large-aperture lens should be used. However, it is important to achieve a good balance between spectrometer performance and the size of the optical system.

Note that the actual resolution depends on the constraint of the pixel resolution of array elements because the outputs from the OCM are discrete data which are sampled by a photodiode array.

DELAY INTERFEROMETER

A delay interferometer demodulates light which is modulated by Differential Phase Shift Keying (DPSK). This device compares phases by interfering with an original optical signal and its 1-bit delayed signal, and then it changes the difference in phases into that of intensity. Figure 6 shows an external view of the 1 × 2 pigtail fiber type delay interferometer to be released. Table 2 lists the main specifications.

Figure 7 shows the optical system of the delay interferometer. Basically, the device is a Mach-Zehnder interferometer, so its lens system is a pseudo confocal system like an OCM.

The two waves that have interfered with each other are Gaussian

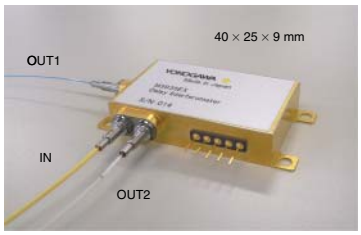

Figure 6 External View of Delay Interferometer

Table 2 Specifications of the Delay Interferometer (for 10 Gbps)

Item	Specification
Wavelength Range	C or L-band (1528.77-1608.33 nm)
Free Spectral Range Error	< 1%
Insertion Loss	< 2.5 dB
Polarization Dependent Loss	< 0.2 dB
Polarization Dependent Frequency Shift	< FSR/100
Tuning Range	> FSR × 2
Dimensions	40 × 25 × 9 mm
Operating Temperature Range	-5 to 70°C

beams, whose wavefronts are spherical. The radius of the beams (ω_2, ω_2') and the radius of curvature of the phase front (R_2, R_2') near the point (on the surface of the non-polarization beam splitter) of the interference of these two beams are shifted by the optical path length. The degree of interference can be estimated by the following formula that gives the combination efficiency in the basic modes of each Gaussian beam[4]:

$$\eta = \frac{4}{\left[\frac{\omega_2}{\omega_2'} + \frac{\omega_2'}{\omega_2}\right]^2 + \left[\frac{\pi \omega_2 \omega_2'}{\lambda}\right]^2 \left[\frac{1}{R_2} - \frac{1}{R_2'}\right]^2} \quad \cdots (10)$$

The value of (ω_2, ω_2') and (R_2, R_2') can be obtained by formula (2). Although the combination efficiency η is shifted by optical path length, it is maximized with value 1 where $\omega_2 = \omega_2'$ and R_2, = R_2'. Using this formula, the ideal excessive loss and extinction ratio can be estimated.

Let ω_2 be the beam waist near the beam splitter and ω_2' be a beam which is diffused in optical path length z = L, then as formula (2) shows, as the value ω_2 becomes larger, the value ω_2' reaches the value ω_2, and R_2' reaches R_2 (infinity). Therefore, increasing the radius of the collimated beam causes the beam fluctuation, which arises from

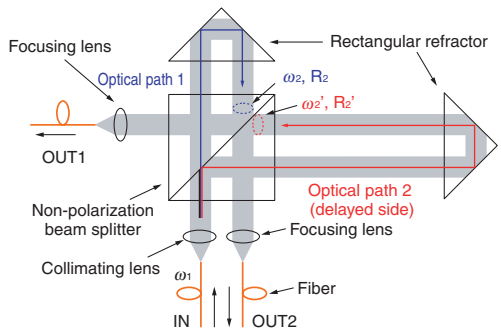

Figure 7 Optical System of Delay Interferometer

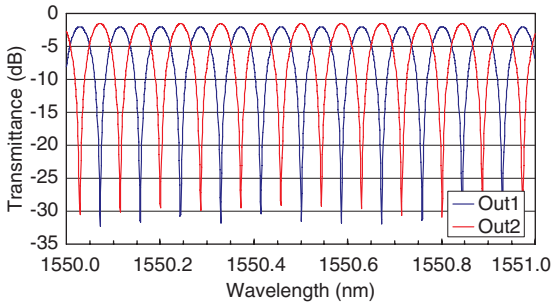

Figure 8 Transmittance of Delay Interferometer

the difference of optical path length, to decrease and the value η increase, thus improving the performance. Like an optical channel monitor, there is a trade-off between the performance of an optical system and its size.

The smaller gap (relative offset) and slope between the beams with different optical path length contribute to the better performance.

Figure 8 shows the input/output characteristics of the delay interferometer, namely the transmission characteristics (real value in measurement) of OUT1 and OUT2. The insertion loss is less than 2.5 dB, and the extinction ratio is more than 25 dB.

CONCLUSION

This paper described the main specifications and analysis examples using a Gaussian beam for the optical system of a compact optical channel monitor and a delay interferometer having free-space optical elements.

The analysis using a Gaussian beam covered the entire optical system, so that we confirmed that it is adequate for a rough design process for determining the basic performance and size of optical systems.

The devices introduced in this paper utilize in optical transmission systems, and there is strong demand for compact, thin and flat devices. Various approaches for miniaturization have been attempted due to the trade-off between the performance of an optical system and its size. There are many other important detailed design issues concerning the lens, thin-film, and so on. In addition, the detailed design must consider the reliability and ease of assembly. We will examine these issues in a later paper. ◆

REFERENCES

(1) Kenichi Iga, "Microoptics," Applied Physics, Vol. 55, No. 7, 1986, pp. 661-669 in Japanese
(2) The Japan Society of Applied Physics:Optical Society of Japan, The Physical Basics of Microoptics (1st Edition), Asakura Publishing, 1991, 222 p. in Japanese
(3) Toshiaki Suhara, Engineering of Optical Waves (1st Edition), Corona Publishing, 1998, pp. 225-229 in Japanese
(4) Kenji Kawano, Basics and Application of Optical Connections (1st Edition), Gendaikougakusya, 1991, 172 p. in Japanese
(5) H. Kogelink, T. Li, "Laser Beams and Resonators," Applied Optics, Vol. 5, No. 10, 1966, pp. 1550-1567